

FLUX BALANCING CONTROL OF NANO CRYSTALLINE CORE BASED TRANSFORMERS WITH DUAL ACTIVE BRIDGE CONVERTER SYSTEM

Donapati R Krishna Reddy¹, Dr. Subhashish Boss²

¹Research Scholar, Dept. of Electrical & Electronics Engineering, Sri Satya Sai University of Technology & Medical Sciences, Sehore, Bhopal-Indore Road, Madhya Pradesh, India

²Research Guide, Dept. of Electrical & Electronics Engineering, Sri Satya Sai University of Technology & Medical Sciences, Sehore, Bhopal Indore Road, Madhya Pradesh, India

Received: 14 March 2020 Revised and Accepted: 8 July 2020

ABSTRACT: Transformer flux dc inclination is a basic issue, impacting the reliable operation of dual active bridge (DAB) converters especially when high permeability nanocrystalline core is used. Steady state current dc inclination can easily saturate nanocrystalline transformers, and it is even more dangerous in transient conditions. A dc predisposition model is proposed to analyze steady state dc inclination in different load conditions. The magnetizing current detection is necessary for closed loop control of dc predisposition, conductors' position is appeared to impact sensor noise. To deal with both steady state and transient dc inclination, a unified flux balancing control (UFBC) is proposed presenting a predictive predisposition suppression (PBS) method with closed-loop flux balancing control (CFBC). A lossless method of tuning the leakage inductance of the transformer, suitable for low-profile nanocrystalline transformer. With the proposed PBS, both essential/secondary current balance and flux balance can be achieved inside one exchanging cycle utilizing UFBC. Power characteristics and interaction between power control and flux balancing control of DAB converters are analyzed, and the CFBC need to work in a low bandwidth due to sensor bandwidth impediment and interaction between power control and flux balancing control.

KEYWORDS: Nanocrystalline, Dual active bridge convertor, Magnetizing current, Transformer Flux, Unified Flux Balancing Control (UFBC), Closed-loop Flux Balancing Control (CFBC), Power control.

I. INTRODUCTION

Today, dual active bridge converters are increasingly discovering applications in power systems with energy-storage capacity, most prominently in "smart"- grid and automotive applications. Generally, they are employed to condition charging and releasing of the energy-storage devices, for example, batteries and super capacitors. Specifically, in automotive applications, isolated bidirectional dc-dc converters are used in electric vehicles (EVs) to provide bidirectional energy exchange between the high voltage (HV) and low-voltage (LV) battery, whereas bidirectional air conditioning dc converters are required for future vehicle-to-grid (V2G) applications. Due to a relatively wide battery-voltage range that is dependent on battery's state of charge, achieving high efficiency over the entire battery voltage range is a significant design challenge of bidirectional dc-dc converters.

With the developing demand of high-flux density power conversion systems, the high-frequency high-power transformers have attracted critical attention in recent years. Operated with a higher frequency, the volume of a magnetic core can be minimized. When the power limit increases, however, advanced delicate magnetic materials of high permeability, high immersion flux densities, and low core losses, nanocrystalline composites can be the excellent choice.

Power electronics transformer (PET) is confronting fast development these days, which pulls in more and more attentions in academia and industry for its powerful density, little size, reduced weight, and low noise. With SiC power devices and nanocrystalline transformer cores used in PET, the exchanging loss of the high frequency converter and the all out loss of the HFIT could be further reduced, which can greatly improve the overall efficiency and the power density of the PET system. Spot is considered as one of the most encouraging topologies of PET in medium and high power applications for its high frequency galvanic seclusion, delicate exchanging control realization, bidirectional energy stream ability, and high reliability. Be that as it may, it is hard to meet the high voltage requirements in some cases like fast railroad foothold system etc. due to the

voltage rating cutoff points of its power exchanging devices used. ISOP cascade topology of multiple DABs can be adopted to solve this problem. Compared with the power devices direct series connected methodology, ISOP topology is easier to achieve measured design and has higher reliabilities. However, the conveyances of the information voltage, the yield current and the transferred power of each DAB in ISOP topology ought to likewise be considered for they are very sensitive to the value of the phase-move inductance.

Dual Active Bridge Converter

A dual active bridge is a bidirectional DC-DC converter with identical essential and secondary side full-bridges, a high frequency transformer, an energy transfer inductor and DC-interface capacitors. Energy transfer inductance in the model refers to the leakage inductance of the transformer in addition to any necessary external energy transfer inductance.

The two legs of both full-bridges are driven with complimentary square-wave pulses. Power stream in the dual active bridge can be directed by phase-moving the pulses of one bridge with respect to the other utilizing phase move tweak. The control directs power between the two DC busses with the end goal that the leading bridge delivers power to the slacking bridge. The applied square waves to the bridges create a voltage differential over the energy transfer inductance and direct its stored energy.

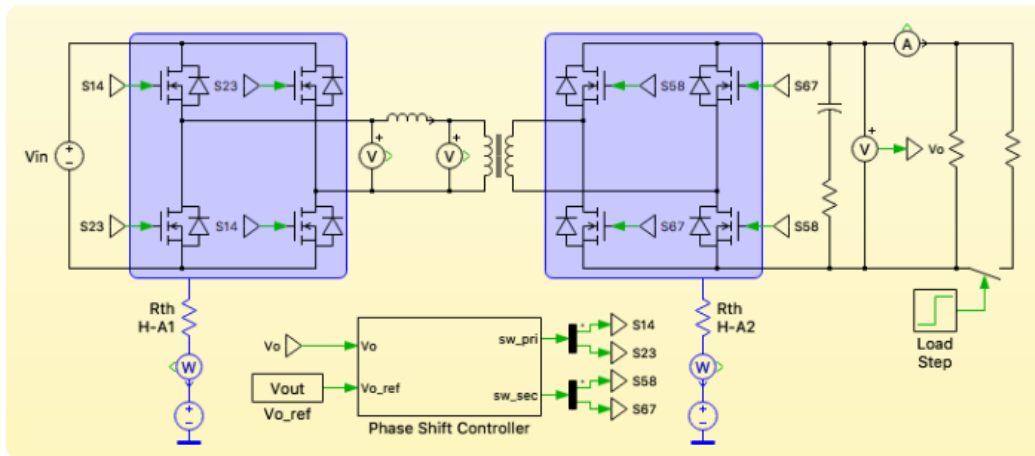


Figure 1: Circuit diagram of DAB converter

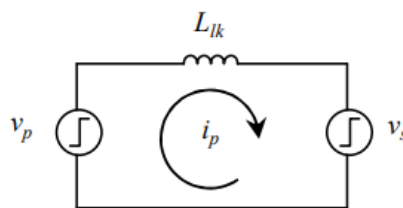


Figure 2: equivalent circuit of DAB converter

In ideal cases with dual active bridge converters, zero voltage switching (ZVS) can be realized when the voltage transfer ratio (M) across the transformer is equal to 1:

$$M = V_{out} \div (n \times V_{in})$$

where, n is the transformer turn ratio

Vout is the output voltage

Vin is the input voltage.

In non-ideal cases, zero voltage exchanging depends on the resonant relationship between the yield capacitance over each device and the equivalent inductance of the circuit during different exchanging intervals. During exchanging events, the current through one of the complimentary devices is interrupted, yet due to the energy transfer inductance, current is supplied through the yield capacitor and forced through the counter parallel diode of the device.

Control

Each switch is on for half of its respective exchanging period. The switch sets in the two bridges all have the same exchanging period however are operated with the end goal that between each bridge a phase move is introduced that varies based on the balance derived from feedback measurements. A yield voltage error signal is generated based on a set point value and this is fed through a computerized PI regulator to generate the phase move proportion for the PWM modulator.

Magnetic Model

The transformer model can be configured as an ideal transformer for speeding up the recreation or as a more detailed transformer model that includes immersion behavior. For the detailed version, Payton Planar Magnetics' T250-4-16 transformer is modeled utilizing the PLECS magnetic area. The parameters of the magnetic model are directly related to the geometry and material characteristics of the core, which by and large can be obtained from datasheets. The transformer uses industry standard E43/28 core and TP4A ferrite material from TDG.

Nanocrystalline Core based Transformer

Nanocrystalline magnetic materials have potential to push the transformer power density and power processing limit higher, because of their high immersion level, low misfortune density, high operation temperature and high thermal conductivity. Since laminated with quickly quenched strips, the majority of nanocrystalline cores in E- or C-shapes for transformer use are assembled massive for enough mechanical strength. Therefore, they gain their ubiquity in high power applications where large cores are normally required. However, the studies about the position of safety nanocrystalline transformer that can be employed in printed circuit board (PCB) based converter is quite rare.

In a high current converter, the high conduction losses in components, like semiconductors and transformer windings, deteriorate the system efficiency altogether. Reduction of the conduction losses in the transformer is one of the essential design issues for this sort of converter. For the commercial ferrite transformer cores, their shapes have been standardized and the space left for the design optimization of different applications is limited. Due to the fragile material properties, it is hard to machine an already-made ferrite core for desired dimensions and embellishment the core will cost a ton. A large portion of the transformer core made of nanocrystalline can be hand crafted, which provides opportunities to optimize the core shapes as indicated by the design needs preceding the assembling. The core dimension optimization towards a base misfortune is proposed for the high-current applications.

Unlike the converters, for example, fly back, the leakage inductance of the transformers ought to be minimized to constrain the voltage spikes. A specific leakage inductance is required in phase-shifted converters, for example, the series resonant full bridge converter and dual active bridge converter. Besides including an external inductor in series to the transformer, several methods can be applied to tune the leakage inductance by increasing the leakage energy inside the cores. But since of the shallow and wide structure, increasing leakage energy inside the proposed high-current nanocrystalline cores isn't an effective method. The best approach to tune the leakage inductance by molding the windings externally to nanocrystalline core is discussed. Following the core dimension optimization and leakage control method, nanocrystalline transformers are designed for a 100 kHz DAB converter with very high transient current.

Table 1: Comparison of Nanocrystalline FT-3M and Ferrite (3C90) materials

Material	Nanocrystalline	Ferrite
	FT-3M	3C90
Bs [T] @ 20 °C	1.23	0.47

T _c [°C]	570	220
μ _r @ 10 kHz	50,000	~2000
density [g/cm ³]	7.3	4.8
σ _{th} [W/m.K]	~9	~4
ρ [Ωm]	1.2x10 ⁻⁶	5

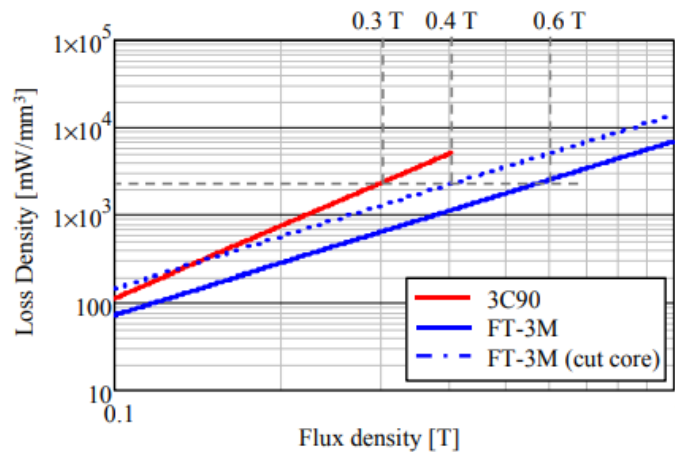


Figure 3: Loss density of 3C90 and FT-3M

Properties of a nanocrystalline material, FT-3M and a ferrite material 3C90, are compared in Table. 1. It is seen that FT-3M is superior in high immersion flux density and high temperature operation capacity. Figure 3 shows the misfortune density of two materials at 100 kHz. FT-3M material is substantially more efficient than 3C90. However, for the cut-cores, like C and E-shaped cores, the core preparation effect exists due to the air cut between cores. This effect approximately doubles the core misfortune density. The misfortune density of cut-core is additionally indicated in Figure 3 (dashed line). It very well may be discovered that to get the same misfortune density level of 3C90 at 0.3 T, the flux density of FT-3M material and cut-core can reach 0.6 T and 0.4 T, which implies larger power-processing capacity of the nanocrystalline core.

III. PROPOSED METHODOLOGY

In this section we are talking about on flux balancing control of Nanocrystalline core based transformers with dual active bridge converter system. One current loop is used to regulate average magnetizing current i_{Mav} to approximately zero to maintain a strategic distance from immersion of the transformer magnetic core, whereas the other control loop is employed to regulate average essential current i_{pav} to approximately zero to prevent unnecessary power misfortune in the essential and secondary side of the converter caused by the dc component of these currents, just as to prevent the eventual immersion of the magnetic core of inductor LAC.

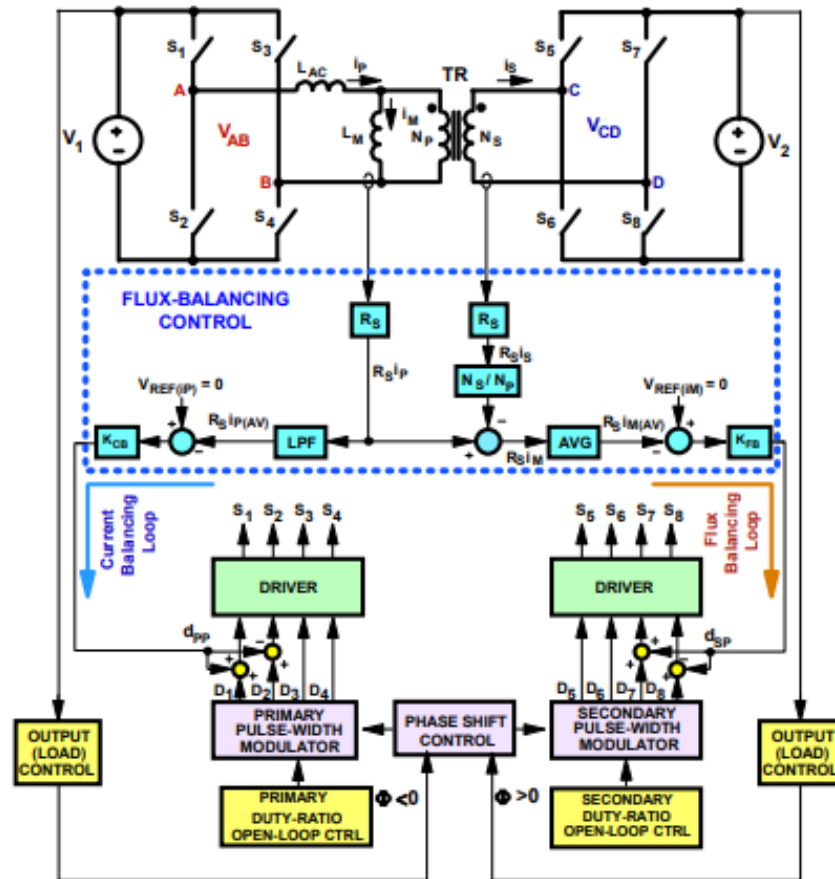


Figure 4 DAB converter: Power stage and control block diagram

The blocks related to proposed transformer flux-balancing control are appeared in Figure. 4 inside the dashed blue rectangle. In Figure. 4, the control of the DAB circuit is implemented with two current-control feedback loops notwithstanding the yield feedback control loops and the essential and secondary-side obligation cycle open-loop control.

Two current loops are needed because the magnetizing current is given by the difference between essential current i_p and scaled secondary current i_s ,

$$i.e) \text{ } a s i_M = i_p - (N_s i_s \div N_p)$$

Where N_P and N_S are the number of turns of the essential and secondary twisting, respectively. Therefore, constraining the average magnetizing current to zero by the magnetizing current control loop does not guarantee that the average essential and secondary currents are likewise zero since the zero value of the average magnetizing current can be achieved with non-zero values of the average essential and secondary currents.

The current loop that regulates the average magnetizing current is implemented by sensing essential current i_P and secondary current i_S by current-sensing devices with gain R_S and deducting the sensed value of the essential current $R_S \cdot i_P$ from the scaled value of the sensed secondary current $(N_S/N_P) \cdot R_S \cdot i_S$ to acquire the sensed value of magnetizing current $R_S \cdot i_M$. Sensed magnetizing current $R_S \cdot i_M$ is then averaged by the AVG square. After the averaging, average sensed magnetizing current $R_S \cdot i_{Mav}$ is compared with reference $V_{REF}(i_M)$ that is set to zero value. The difference between the average sensed magnetizing current and its reference is further processed by controller K_{FB} whose yield modulates the obligation cycles of the complementary switched same-leg secondary-side switches S_7 and S_8 so the value of sensed magnetizing current $R_S \cdot i_{Mav}$ is maintained at approximately zero.

The complementary adjustment of the obligation cycle of secondary side switches S_7 and S_8 , appeared in Figure. 4 i.e., the change of the obligation cycle of switch S_7 by sum d_{SP} and a simultaneous change of the

obligation cycle of the same-leg switch S8 for an equal measure of the opposite sign, - dSP, causes the regulation of obligation cycle of positive bridge voltage VCDP, as illustrated in Figure 5. As can be seen in Figure. 5 during half-periods of negative bridge voltage VCDN no balance takes place. With this one-sided tweak, the control can change the positive volt-second product over the secondary winding and, therefore, magnetizing inductance, to balance the flux between the positive and negative half-periods, i.e., to keep up the average magnetizing current approximately at zero

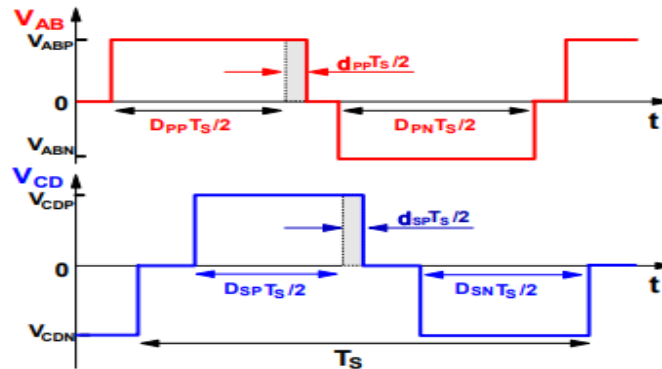


Figure. 5 Modulation of primary and secondary bridge voltages VAB and VCD to implement proposed flux-balancing control.

The current loop that regulates the average essential current is implemented by averaging sensed essential current $RS \cdot i_P$ by low pass filter (LPF) obstruct in Figure 6. After the averaging, average sensed essential current $RS \cdot i_{pav}$ is compared with reference $V_{REF}(i_P)$ that is set to zero value. The difference between the average sensed essential current and its reference is further processed by controller KCB whose yield modulates the obligation cycles of the complementary-switched same-leg essential side switches S3 and S4 with the goal that the value of sensed essential current $RS \cdot i_{pav}$ is maintained at approximately zero. It ought to be noted that by keeping up both the average magnetizing and essential current close to zero by the two-current-loop control, the average secondary current, which is relative to the difference between these two currents, is likewise kept close to zero.

To be effective in preventing transformer immersion, the flux balancing loop that keeps the average magnetizing current to approximately zero must be very quick. It ought to be designed with the maximum possible loop bandwidth since the loop must respond to any transformer core flux imbalances as quick as could reasonably be expected. The bandwidth of the essential current balancing loop that eliminates the dc component of the essential current might be a lot of lower than that of the flux-balancing loop since essential inductor LAC is designed to convey generous dc current without soaking its magnetic core. By having the bandwidths of two current-control loops well separated, the interaction between the two loops is basically eliminated which enhances the robustness of the control.

At long last, it ought to be noted that the bandwidths of the yield feedback loops should likewise be well separated from the bandwidths of the two current loops to evade undesirable loop interactions. Therefore, the bandwidths of the yield loops ought to be placed well below the bandwidth of the quick flux-balancing control loop and well above the bandwidth of the moderate current balancing loop.

IV. RESULT

Along these lines the flux is balanced by utilizing Nano crystalline core based transformers with dual active bridge converter system. The performance and parameter of Nano crystalline transformers of FT-3H and FT-3M materials are summarized in Table 2.

Table 2: Optimal parameters of high-frequency transformers with different magnetic materials

Material	Nanocrystalline	
	FT-3H	FT-3M
Core losses (W)	3.948	3.637
Winding losses (W)	1.798	1.759
Total losses (W)	5.7459	5.396
Volume (cm ³)	48.13	49.26
Weight (kg)	0.349	0.357
Efficiency (%)	99.809	99.82

The flux density of core and the voltage and current of essential and secondary windings for Nano crystalline transformers is demonstrated as follows.

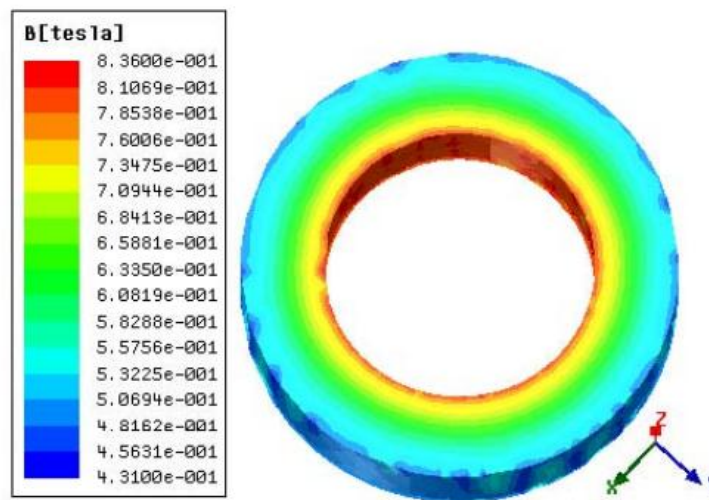


Figure 6 Flux distribution of Nanocrystalline core

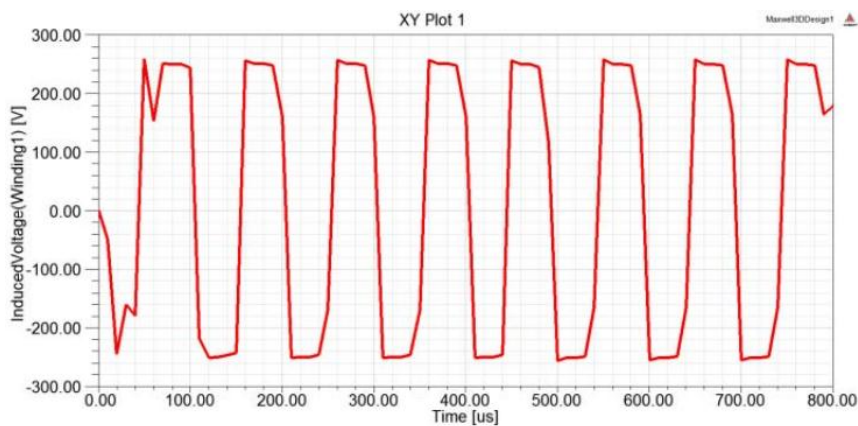


Figure 7 Excitation voltage of primary winding.

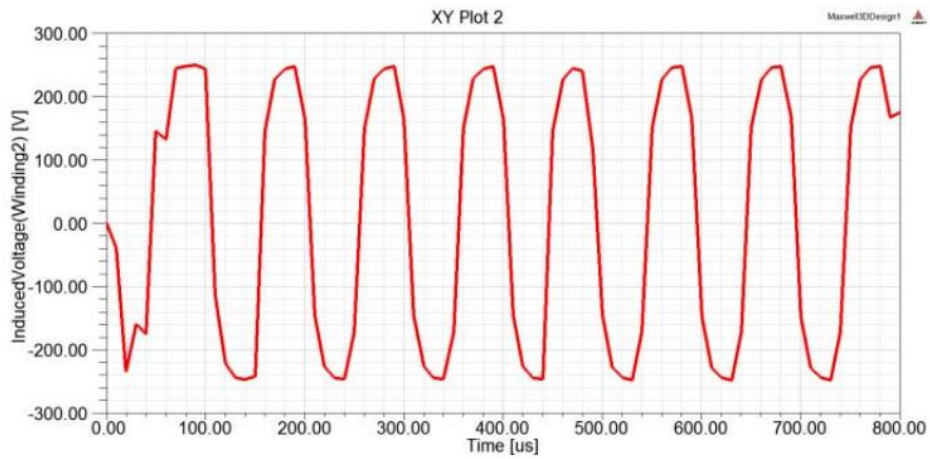


Figure 8 Induced voltage of secondary winding

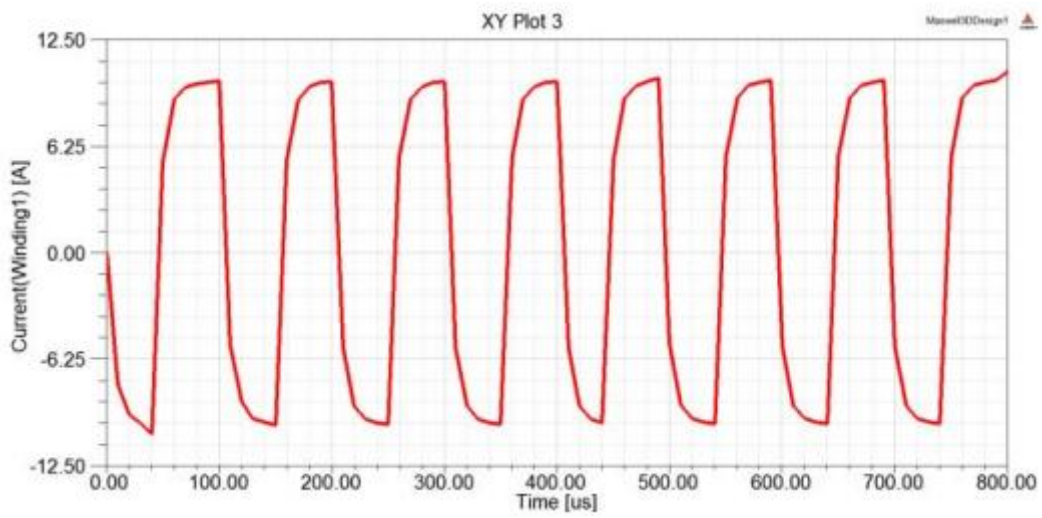


Figure 9 Current in primary winding.

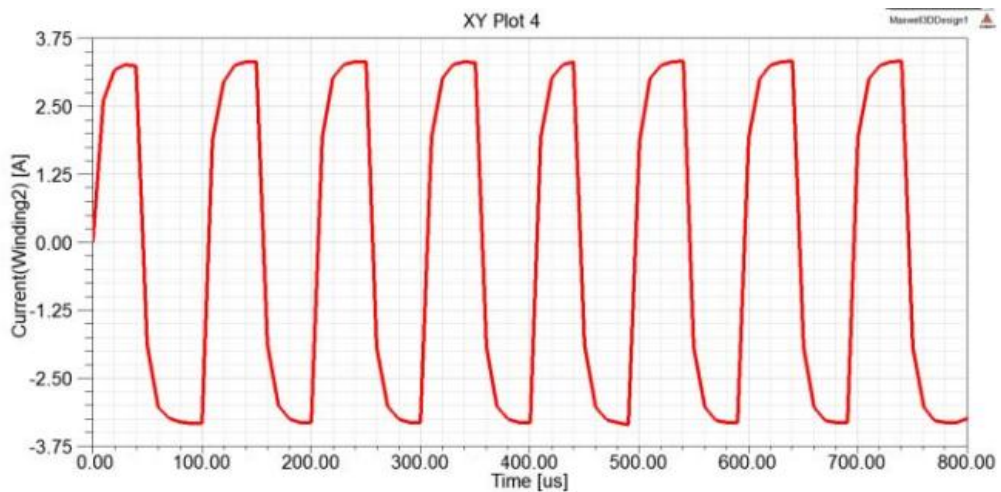


Figure 10 Current in the secondary windings

V. CONCLUSION

The paper proposed a flux-balancing method for the dual active-bridge converter based on direct control of the magnetizing current. In the proposed method, the dc components of the essential and secondary current are controlled by two feedback loops. The objective of the principal loop is to keep up the average magnetizing current at approximately zero level, whereas the purpose of the other loop is to keep the average essential and secondary currents close to zero. Due to low immersion current of nanocrystalline core transformer, it tends to be saturated in steady state. To be effective in preventing transformer immersion, the flux-balancing loop that keeps the average magnetizing current to approximately zero must be very quick. Compared to conventional methods, accurate steady state dc inclination control can be achieved with UFBC, meeting requirement of low immersion current, while a very quick powerful can even now be achieved, without impacting dependability of flux balance closed-loop control.

VI. REFERENCES

- [1] D. Nguyen, K. Yukita, G. Fujita and M. C. Ta, "A simple DC bias elimination technique for Dual-Active-Bridge DC/DC converters," in Proc. International Conf. on Power Electron. and ECCE Asia, Busan, Korea (South), 2019, pp. 1-6.
- [2] Herzer, Giselher. "Modern soft magnets: Amorphous and nanocrystalline materials." *Acta Materialia*, vol. 61, no. 3, pp. 718-734, Feb. 2017
- [3] Y. Yao, S. Xu, W. Sun, S. Lu, "A novel compensator for eliminating DC magnetizing current bias in hybrid modulated dual active bridge converters." *J. Power Electron.*, vol. 16, no. 5, pp. 1650-1660, Sep. 2016.
- [4] Y. Panov, M. M. Jovanović and B. T. Irving, "Novel transformer-fluxbalancing control of dual-active-bridge bidirectional converters," in Proc. IEEE Appl. Power Electron. Conf. Expo., 2015, pp. 42-49.
- [5] B. Zhao, Q. Song, W. Liu and Y. Sun, "Overview of Dual-Active-Bridge Isolated Bidirectional DC–DC Converter for High-Frequency-Link Power-Conversion System," *IEEE Trans. Power Electron.*, vol. 29, no. 8, pp. 4091-4106, Aug. 2014.
- [6] S. P. Engel, N. Soltau, H. Stagge and R. W. De Doncker, "Dynamic and Balanced Control of Three-Phase High-Power Dual-Active Bridge DC-DC Converters in DC-Grid Applications," in *IEEE Transactions on Power Electronics*, vol. 28, no. 4, pp. 1880-1889, April 2013.
- [7] N. M. L. Tan, T. Abe, and H. Akagi, "Design and Performance of a Bidirectional Isolated Dc-Dc Converter for a Battery Energy Storage System," *IEEE Trans. Power Electronics*, vol. 27, no. 3, Mar. 2012, pp. 1237-1248
- [8] F. Krismer and J.W. Kolar, "Efficiency-Optimized High-Current Dual Active Bridge Converter for Automotive Applications," *IEEE Trans. Industrial Electronics*, vol. 59, no. 7, Jul. 2012, pp. 2745-2760
- [9] Dhuha Khalid Alferidah, NZ Jhanjhi, A Review on Security and Privacy Issues and Challenges in Internet of Things, in *International Journal of Computer Science and Network Security IJCSNS*, 2020, vol 20, issue 4, pp.263-286
- [10] Almusaylim Z, Alhumam A, Mansoor W, Chatterjee P, Jhanjhi NZ. Detection and Mitigation of RPL Rank and Version Number Attacks in Smart Internet of Things. Preprints.org; 2020
<https://doi.org/10.20944/preprints202007.0476.v1>
- [11] Vahini Ezhilraman S., Srinivasan S., **Suseendran G.** (2020) "Gaussian Light Gradient Boost Ensemble Decision Tree Classifier for Breast Cancer Detection", In: Peng SL., Son L., Suseendran G., Balaganesh D. (eds) *Intelligent Computing and Innovation on Data Science. Lecture Notes in Networks and Systems*, Vol 118. Pages 31-38 Url : https://link.springer.com/chapter/10.1007/978-981-15-3284-9_4
- [12] Josephine Isabella S., Srinivasan S., **Suseendran G.** (2020) An Efficient Study of Fraud Detection System Using MI Techniques. In: Peng SL., Son L., Suseendran G., Balaganesh D. (eds) *Intelligent Computing and Innovation on Data Science. Lecture Notes in Networks and Systems*, Vol 118 Pages 59-67. Url : https://link.springer.com/chapter/10.1007/978-981-15-3284-9_8
- [13] G. Ortiz, J. Mühlethaler, and J. W. Kolar, "Magnetic Ear"-Based Balancing of Magnetic Flux in High Power Medium Frequency Dual Active-Bridge Converter Transformer Cores," *Proc. IEEE 8th International Conference on Power Electronics, ECCE Asia*, pp. 1307- 1314, 2011
- [14] M. Kheraluwala, R. Gascoigne, D. Divan, and E. D. Baumann, "Performance Characterization of a High-Power Dual Active Bridge Dcto-Dc Converter," *IEEE Trans. Industry Applications*, vol. 28, no. 6, Nov./Dec. 1992, pp. 1294-1301